

Pinning down the leptophobic Z' in leptonic final states with Deep Learning

Tanumoy Mandal,^{1,*} Aniket Masaye,¹ Subhadip Mitra,^{2,†} Cyrin Neeraj,^{2,‡} Naveen Reule,^{1,§} and Kalp Shah^{2,¶}

¹Indian Institute of Science Education and Research Thiruvananthapuram, Vithura, Kerala, 695 551, India

²Center for Computational Natural Sciences and Bioinformatics,

International Institute of Information Technology, Hyderabad 500 032, India

(Dated: July 4, 2023)

A leptophobic Z' that does not couple with the Standard Model leptons can evade the stringent bounds from the dilepton-resonance searches. In our earlier paper [T. Arun *et al.*, Search for the Z' boson decaying to a right-handed neutrino pair in leptophobic $U(1)$ models, *Phys. Rev. D*, **106** (2022) 095035; [arXiv:2204.02949](https://arxiv.org/abs/2204.02949)], we presented two gauge anomaly-free $U(1)$ models where a heavy leptophobic Z' is present along with right-handed neutrinos (N_R). We pointed out the interesting possibility of a correlated search for Z' and N_R at the LHC through the $pp \rightarrow Z' \rightarrow N_R N_R$ channel. This channel can probe a part of the leptophobic Z' parameter space that cannot be otherwise probed using the standard dijet resonance searches. In this paper, we analyse the monolepton final state arising from the decay of the N_R pair. We show that a leptophobic Z' as heavy as 7 TeV and with a gauge coupling of the order of the electroweak coupling is discoverable through this channel at the high-luminosity LHC.

I. INTRODUCTION

Many extensions of the Standard Model (SM), like the grand unified theories (GUTs) [1–3], contain an electrically neutral colour-singlet heavy gauge boson, Z' . To get such a particle in the spectrum, one can simply add an extra local $U(1)$ symmetry spontaneously broken by a complex scalar field with a TeV-scale vacuum expectation value in a bottom-up approach. The phenomenology of a TeV-scale Z' is well-explored in the literature (see, e.g., [4, 5]). One of the current programs of the LHC is to look for the signature of Z' . However, so far, the focus has been only on the cases where it decays exclusively to the SM particles [6–14]. The failure to find the Z' in the SM-decay modes motivates us to look for other possibilities with *non-standard* decay modes of Z' , i.e., where it can decay to beyond-the-SM (BSM) particles as well.

One interesting possibility is when the Z' decays to a pair of right-handed neutrinos (RHNs, N_R) [15–19]. While appending an additional $U(1)$ gauge symmetry to the SM group, one must ensure the cancellation of all gauge anomalies to maintain gauge invariance and renormalizability of the theory. To cancel the gauge anomalies, one can include RHNs in the particle spectrum [20] or rely on some special mechanism like the Green-Schwarz (GS) mechanism [21, 22]. Therefore, many anomaly-free $U(1)$ extensions of the SM contain RHNs since they can also help generate light neutrino masses through various seesaw mechanisms.

The strongest exclusion limits on the Z' parameter space usually come from the dilepton resonance searches [8, 9]. For instance, the current mass exclusion limit on a sequen-

tial Z' is about 5 TeV [8]. The stringent dilepton exclusion limits can be evaded if the Z' is leptophobic, i.e., it does not couple (or couples very feebly) to the SM leptons. In the leptophobic case, the nonstandard decay modes of the Z' become especially important if the branching ratios (BRs) to the new modes are high. In our previous paper [23], we presented two theoretically well-motivated leptophobic Z' scenarios where the Z' dominantly decays to a pair of RHNs. Being leptophobic, these scenarios can easily bypass the spillover dilepton exclusion limits. At the same time, a large BR of the $Z' \rightarrow N_R N_R$ decay and the subsequent decays of N_R to $W\ell$, $Z\nu$, and $H\nu$ final states open up many interesting leptonic final states (see, e.g., Fig. 1). The process $pp \rightarrow Z' \rightarrow N_R N_R$ is not only important from the Z' -search point of view but for the RHN searches as well. Since RHNs are SM singlets, producing them at the LHC is difficult as their production cross sections are small, suppressed by the light-heavy neutrino mixing angles. However, they can be copiously produced if they come from the decays of another BSM particle [24–27].

The RHN pair production from the decay of the Z' has been previously discussed in some phenomenology papers [15–19]. We considered this channel in a leptophobic setup and estimated the high-luminosity LHC (HL-LHC) reach with a simple cut-based analysis in Ref. [23]. Interestingly, we found that a large chunk of the parameter space beyond the reach of $pp \rightarrow Z' \rightarrow jj$ can be probed through the $pp \rightarrow Z' \rightarrow N_R N_R$ channel at the HL-LHC. The decay of the RHN pair can lead to multilepton final states. There we considered the dilepton channel (which is easy to handle in a cut-based analysis and has a good sensitivity) to estimate the HL-LHC reach. The monolepton mode is complementary but more challenging because of the difficulty in the background reduction. In this paper, we estimate the reach in the monolepton final state with a deep neural network (DNN) model.

The RHNs we consider here are around the TeV scale, much lighter than the standard type-I seesaw scale $\sim 10^{14}$ GeV. To naturally realise the TeV-scale RHNs, we con-

* tanumoy@iisertvm.ac.in

† subhadip.mitra@iiit.ac.in

‡ cyrin.neeraj@research.iiit.ac.in

§ naveenreule20@iisertvm.ac.in

¶ kalp.shah@research.iiit.ac.in

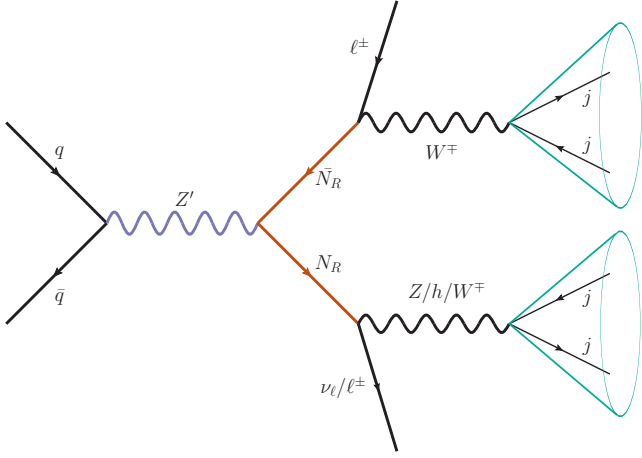


FIG. 1. Representative Feynman diagram for a leptophobic Z' decaying to two right-handed neutrinos.

sider inverse-seesaw mechanism (ISM) for neutrino mass generation [28, 29]. As a result, unlike the Majorana type RHNs in the type-I seesaw, the RHNs here are pseudo-Dirac in nature. Earlier, in Refs. [30–34], different $U(1)$ extensions using the ISM were considered in various contexts. Also, the future lepton colliders could be the best testing ground for the heavy neutrinos [35–37].

II. LEPTOPHOBIC Z' MODELS

We look at the two examples of anomaly-free gauge extensions of the SM from Ref. [23], where a leptophobic Z' with substantial $Z' \rightarrow N_R N_R$ branchings is present. In one example, the RHNs cancel the mixed gauge-gravity anomaly while the GS mechanism cancels the rest, while in the other, the leptophobia of Z' arises in a GUT framework [38–41]. Below, for completeness, we revisit the essential details of these two examples of leptophobic constructions.

A. GS mechanism and leptophobia

In this case, the particle spectrum includes three RHNs—one for every generation—equally charged under the extra $U(1)_z$. The light-neutrino masses are generated through the ISM for which there is also an extra chiral sterile fermion S_L introduced for every generation. We show the $U(1)_z$ charges of various fields in Table I. The charge assignment is generation independent. The SM leptons are uncharged under $U(1)_z$ to make the Z' leptophobic. The nonzero $U(1)_z$ charges of the quarks ensure the Z' can be produced at the LHC through quark-quark fusion. Here, $U(1)_z$ quark charges are kind of arbitrary, and other choices are also possible. The SM Higgs doublet is chargeless under $U(1)_z$ to minimise the mixing between Z and Z' . The scalar ϕ with unit $U(1)_z$ charge is the flavon field introduced to

TABLE I. Particle representations and quantum numbers in the GS extension.

	$SU(3)_c$	$SU(2)_L$	$U(1)_Y$	$U(1)_z$
Q_L	3	2	1/3	z_q
u_R	$\bar{\mathbf{3}}$	1	4/3	$-z_q$
d_R	$\bar{\mathbf{3}}$	1	-2/3	$-z_q$
ℓ_L	1	2	-1	0
e_R	1	1	-2	0
N_R	1	1	0	z_N
H	1	2	1	0
ϕ	1	1	0	1
S_L	1	1	0	0

write down the Yukawa interactions of the SM fermions as shown in Eq. (5). The fermion mass terms arise after the ϕ and H get vacuum expectation values.

The above charge assignment leads to six anomalous triangle diagrams proportional to the traces of the product of the generators as follows:

1. $[SU(3)_C]^2[U(1)_z]$: $\text{tr}[\mathcal{T}^a \mathcal{T}_z^b] = 12z_q$,
2. $[SU(2)_L]^2[U(1)_z]$: $\text{tr}[T^a T_z^b] = 6z_q$,
3. $[U(1)_z]^3$: $\text{tr}[z^3] = 12z_q^3 - z_N^3$,
4. $[U(1)_Y]^2[U(1)_z]$: $\text{tr}[Y^2 z] = 22z_q/3$,
5. $[U(1)_Y][U(1)_z]^2$: $\text{tr}[Y z^2] = 0$,
6. $[R]^2[U(1)_z]$: $\text{tr}[z] = 12z_q - z_N$.

We assume that mixed gauge-gravity anomaly vanishes at low energy and set

$$12z_q - z_N = 0, \quad (1)$$

by hand. Thus, we only have one free charge in our model.

To cancel the other anomalies with the Green-Schwarz (GS) mechanism [42, 43], we add new gauge-dependent terms in the Lagrangian with carefully chosen coefficients. The Peccei-Quinn terms for the mixed anomalies and the $[U(1)_z]^3$ anomaly are written as

$$\begin{aligned} \mathcal{L}_{\text{PQ}} = \frac{1}{96\pi^2} \left(\frac{\Theta}{M} \right) \epsilon_{\mu\nu\rho\sigma} & \left[g_z^2 \mathcal{C}_{zzz} F_z^{\mu\nu} F_z^{\rho\sigma} + g_z g' \mathcal{C}_{zzy} F_z^{\mu\nu} F_Y^{\rho\sigma} \right. \\ & + g'^2 \mathcal{C}_{zyy} F_Y^{\mu\nu} F_Y^{\rho\sigma} + g^2 \mathcal{D}_2 \text{tr} (F_W^{\mu\nu} F_W^{\rho\sigma}) \\ & \left. + g_S^2 \mathcal{D}_3 \text{tr} (F_S^{\mu\nu} F_S^{\rho\sigma}) \right]. \end{aligned} \quad (2)$$

Under the new $U(1)_z$, the pseudoscalar (Goldstone) axion Θ transforms as $\Theta \rightarrow \Theta + M g_z \theta_z$ and the new gauge field transforms as $B_z^\mu \rightarrow B_z^\mu - \partial^\mu \theta_z$. Here, M is the scale at which $U(1)_z$ breaks through the Stückelberg mechanism, F_z, F_Y, F_W, F_S are the field strengths and g_z, g', g, g_S are the coupling constants associated with

the $U(1)_z$, $U(1)_Y$, $SU(2)_L$, $SU(3)_c$ gauge groups, respectively. The generalised Chern-Simons (GCS) terms for other mixed anomalies are given as

$$\mathcal{L}_{\text{GCS}} = \frac{1}{48\pi^2} \varepsilon_{\mu\nu\rho\sigma} \left[g'^2 g_z \mathcal{E}_{zyy} B_Y^\mu B_z^\nu F_Y^{\rho\sigma} + g'^2 g_z \mathcal{E}_{zzy} B_Y^\mu B_z^\nu F_Z^{\rho\sigma} + g^2 g_z \mathcal{K}_2 B_z^\mu \Omega_W^{\nu\rho\sigma} + g^2 g_z \mathcal{K}_3 B_z^\mu \Omega_S^{\nu\rho\sigma} \right] \quad (3)$$

with

$$\Omega_{G,W}^{\nu\rho\sigma} = \frac{1}{3} \text{tr} \left[A_{G,W}^\nu \left(F_{G,W}^{\rho\sigma} - [A_{G,W}^\rho, A_{G,W}^\sigma] \right) + (\text{cyclic permutations of } \rho, \sigma, \nu) \right]$$

and $A_X = [G, W_X]$. The coefficients \mathcal{C} , \mathcal{D} , \mathcal{E} , and \mathcal{K} can be solved in terms of the $U(1)_z$ charges of the fermions as

$$\begin{aligned} \mathcal{E}_{zzz} &= - (12z_q^3 - z_N^3), \\ \mathcal{E}_{zyy} &= -22z_q = \frac{3}{2} \mathcal{E}_{zyy}, \\ \mathcal{E}_{zzy} &= 0 = \mathcal{E}_{zzy}, \\ \mathcal{D}_2 &= -18z_q = -\frac{3}{2} \mathcal{K}_2, \\ \mathcal{D}_3 &= -36z_q = -\frac{3}{2} \mathcal{K}_3. \end{aligned} \quad (4)$$

so that the anomalies are cancelled. The $U(1)_z$ invariant Yukawa interactions are written as

$$\mathcal{L}_Y \supset -\lambda_u \left(\frac{\phi}{\Lambda} \right)^{2z_q} \overline{Q}_L \tilde{H} u_R - \lambda_d \left(\frac{\phi}{\Lambda} \right)^{2z_q} \overline{Q}_L H d_R + h.c., \quad (5)$$

where $\tilde{H} = i\sigma_2 H^*$, and λ_u and λ_d are the Yukawa couplings. After the spontaneous breaking of the $U(1)_z$ symmetry, ϕ acquires a vacuum expectation value $v_\phi = \langle \phi \rangle$ leading to the SM Yukawa terms. The neutrino masses are generated by the ISM through the following higher-dimensional operators,

$$\begin{aligned} \mathcal{L}_Y \supset -\lambda_{ij}^v \left(\frac{\phi^\dagger}{\Lambda} \right)^{z_N} \overline{L}^i \tilde{H} N_R^j - M_{Rij} \left(\frac{\phi}{\Lambda} \right)^{z_N} \overline{N}_R^i S_L^j \\ - \frac{\mu}{2} \overline{S}_L^c S_L + h.c. \end{aligned} \quad (6)$$

We get the mass matrix for the neutrinos after the sequential breaking of the $U(1)_z$ and electroweak symmetries in the $(\nu_L^c N_R S_L^c)^T$ basis as,

$$\mathbf{M}_\nu = \begin{pmatrix} 0 & \mathbf{m}_D & 0 \\ \mathbf{m}_D^T & 0 & \mathbf{M}_R \\ 0 & \mathbf{M}_R^T & \mu \end{pmatrix}, \quad (7)$$

where $\mathbf{m}_D = \lambda^v v_h$, μ , and \mathbf{M}_R are 3×3 mass matrices in the generation space in general. The parameter μ is typically associated with lepton number violation and restores the lepton number symmetry in the $\mu \rightarrow 0$ limit. After diagonalising the matrix in Eq. (7), we get the active (light) neutrino mass matrix as [44],

$$\mathbf{m}_\nu = \mathbf{m}_D \mathbf{M}_R^{-1} \mu (\mathbf{M}_R^T)^{-1} \mathbf{m}_D + \mathcal{O} \left(\frac{1}{\mathbf{M}_R^4} \right). \quad (8)$$

TABLE II. Quantum numbers and representations of the particles contained in the **27** representation of E_6 in the standard embedding. Other fields in the **27** representation are not shown here as they do not play any role in our analysis.

Particle	$SU(3)_c$	$SU(2)_L$	$2\sqrt{6}Q_\psi$	$2\sqrt{10}Q_\chi$	Y
Q_L	3	2	1	-1	1/6
u_R^c	$\overline{\mathbf{3}}$	1	1	-1	-2/3
d_R^c	$\overline{\mathbf{3}}$	1	1	3	1/3
ℓ_L	1	2	1	3	-1/2
e_R^c	1	1	1	-1	1
N_R^c	1	1	1	-5	0

There is a double suppression of the light neutrino masses from the large \mathbf{M}_R (taken around the TeV scale) and the small μ .

B. Leptophobia in E_6 GUT models

In some E_6 GUT models, leptophobia can be realised through gauge-boson kinetic mixing [38] even though the fermion couplings to the gauge bosons are not arbitrary free parameters. In such models, the $U(1)_z$ group can come from a symmetry-breaking chain like,

$$\begin{aligned} E_6 &\rightarrow SO(10) \times U(1)_\chi \\ &\rightarrow SU(5) \times U(1)_\chi \times U(1)_\psi \\ &\rightarrow SU(2)_L \times U(1)_Y \times U(1)_z \\ &\rightarrow SU(2)_L \times U(1)_Y. \end{aligned} \quad (9)$$

The $U(1)_z$ appears as a linear combination of $U(1)_\psi$ and $U(1)_\chi$. The $U(1)_z$ charge Q_z can be expressed as $Q_z = Q_\psi \cos \theta - Q_\chi \sin \theta$ where θ is the E_6 mixing angle. However, there is no solution for θ where the lepton couplings vanish. Therefore, we look at the gauge-kinetic mixing

TABLE III. Q_ψ and Q_χ charges of the ℓ_L and e_R^c for the six embeddings of the leptons in the **27** representation of E_6 , and values of $\tan \theta$ and δ for which leptophobia is realised [41].

Model	ℓ_L		e_R^c		$\tan \theta$	δ
	$2\sqrt{6}Q_\psi$	$2\sqrt{10}Q_\chi$	$2\sqrt{6}Q_\psi$	$2\sqrt{10}Q_\chi$		
1	1	3	1	-1	$\sqrt{3/5}$	-1/3
2	-2	-2	1	-1	$\sqrt{3/5}$	-1/3
3	1	3	1	-5	$\sqrt{15}$	$-\sqrt{10}/3$
4	-2	-2	1	-5	$\sqrt{5/27}$	$-\sqrt{5}/12$
5	1	3	4	0	$\sqrt{5/3}$	$-\sqrt{5}/12$
6	-2	-2	4	0	0	$-\sqrt{10}/3$

terms allowed by the gauge invariance,

$$\mathcal{L}_{kin} \supset -\frac{1}{4}\tilde{F}_Y^{\mu\nu}\tilde{F}_{Y\mu\nu} - \frac{1}{4}\tilde{F}_z^{\mu\nu}\tilde{F}_{z\mu\nu} - \frac{\sin\chi}{2}\tilde{F}_{Y\mu\nu}\tilde{F}_z^{\mu\nu}. \quad (10)$$

The kinetic mixing, parametrised by $\sin\chi$, can be removed by a unitary transformation [40]:

$$\tilde{B}_Y^\mu = B_Y^\mu - \tan\chi B_z^\mu, \quad \tilde{B}_z^\mu = \frac{B_z^\mu}{\cos\chi}. \quad (11)$$

This transformation makes the kinetic mixing vanish only at a particular scale, implying that the mixing term can regenerate at higher orders. This makes the couplings energy-dependent. Hence, they must be evaluated at the TeV scale before relating to the experiments. After the rotation, the couplings of the gauge bosons with the fermions are given as [40],

$$\mathcal{L}_{int} \supset -\bar{\Psi}\gamma_\mu \left[g'Y_{SM}B_Y^\mu + g_z \left(Q_z + \sqrt{\frac{3}{5}}\delta Y_{SM} \right) B_z^\mu \right] \Psi, \quad (12)$$

where $\delta = -\tilde{g}_Y \sin\chi / \tilde{g}_z$. Now the fermion couplings are functions of two free parameters θ and δ , we can in general make the couplings of any two fields vanish. For the standard embedding (Table II), leptophobia corresponds to $\theta = \tan^{-1} \sqrt{3/5}$ and $\delta = -1/3$ [41]. However, as shown in Table III, different combinations of θ and δ work in different embeddings.

III. COLLIDER ANALYSIS

For the collider analysis, we use the following simplified Lagrangian

$$\mathcal{L} \supset \frac{g_z}{2} (z_u \bar{u}_i \gamma^\mu u_i + z_u \bar{d}_i \gamma^\mu d_i + z_N \bar{N}_R \gamma^\mu N_R) Z'_\mu, \quad (13)$$

where $z_{u,d}$ are the effective $U(1)_z$ charges of up and down type quarks where for any quark q it is defined as $z_q^2 = z_{qL}^2 + z_{qR}^2$. We use FEYNRULES [46] to build the above model and obtain the Universal FeynRules Output (UFO). We simulate the hard scattering in MADGRAPH5 [47], showering and hadronisation in PYTHIA [48] and the LHC detector environment in DELPHES3 [49]. The events are generated at $\sqrt{s} = 14$ TeV. Jets are clustered using the anti- k_T algorithm [50] with $R = 0.4$ (we call them as AK-4 jet). For the electron, the DeltaRMax parameter in the DELPHES card (distance between the other isolated objects and the identified electron) for isolation has been modified to 0.2 from 0.5.

A. Event selection criteria

We show the signal topology in Fig. 1. In this paper we focus on the monolepton signature:

$$pp \rightarrow Z' \rightarrow N_R N_R \rightarrow \ell_\mu + \cancel{E} + \text{jets}$$

which arises when one of the RHNs decays to a hadronically decaying W boson and a lepton, while the other decays to a Z/H boson and a neutrino. We look at Z' masses between 3–7 TeV and RHNs ranging from 0.5 to 3.5 TeV. From the topology and the distributions of the final state, we design the following basic selection criteria for the signal events:

- \mathcal{C}_1 : $H_T > 750$ GeV, where H_T is the scalar sum of the transverse momenta of all hadronic objects in an event.
- \mathcal{C}_2 : Exactly one muon, with $p_T > 120$ GeV with $|\eta| < 2.5$.
- \mathcal{C}_3 : At least three AK-4 jets. We also demand that the leading jet has $p_T > 120$ GeV.
- \mathcal{C}_4 : Exactly two fatjets, clustered using the anti- k_T algorithm with $R = 0.7$ and $p_T > 200$ GeV with mass $M_J \in [40, 165]$.
- \mathcal{C}_5 : The invariant mass between the reconstructed muon and missing transverse energy (\cancel{E}_T) must be greater than 140 GeV, i.e., $M_{\mu\cancel{E}_T} > 140$ GeV.

We pick the fatjet radius $R = 0.7$ after optimising to tag a boosted two-pronged jet. The constraints on fatjet mass (\mathcal{C}_4) are chosen to include reconstructed W , Z and H fatjets. Since the missing energy and muon come from the decay of W -boson in all of the backgrounds, we put a high cut on the invariant mass of reconstructed lepton and missing transverse energy pair in \mathcal{C}_5 .

B. Background processes

The major backgrounds considered for the analysis are listed in Table IV, along with the cut efficiencies and the total number of events at the HL-LHC luminosity, 3 ab^{-1} . To reduce the computation time, we generate the background events with some generation-level cuts. The $W^\pm + \text{jets}$ process is the leading background before the cuts; the demand of a high- p_T jet (\mathcal{C}_3) and two fatjets (\mathcal{C}_4) reduces this background significantly. The contributions from the $W^+W^- + \text{jets}$ process drop drastically with the demand of two fatjets (\mathcal{C}_4). The fatjet criterion (\mathcal{C}_4) also cuts the $t\bar{t} + \text{jets}$ background as most of these events have just one fatjet. The hadronically-decaying top is sometimes reconstructed as the fatjet in a fraction of $t\bar{t} + \text{jets}$ events, the demand on the fatjet mass cuts down these events. After the event selection criteria are enforced, $W^+W^- + \text{jets}$ and $t\bar{t} + \text{jets}$ become the leading backgrounds.

C. Kinematic picture

We use the kinematic information of the identified objects, i.e., one muon, three AK-4 jets, and two fatjets, along with some derived quantities to create the input set of variables for the multivariate analysis—the full list of variables is

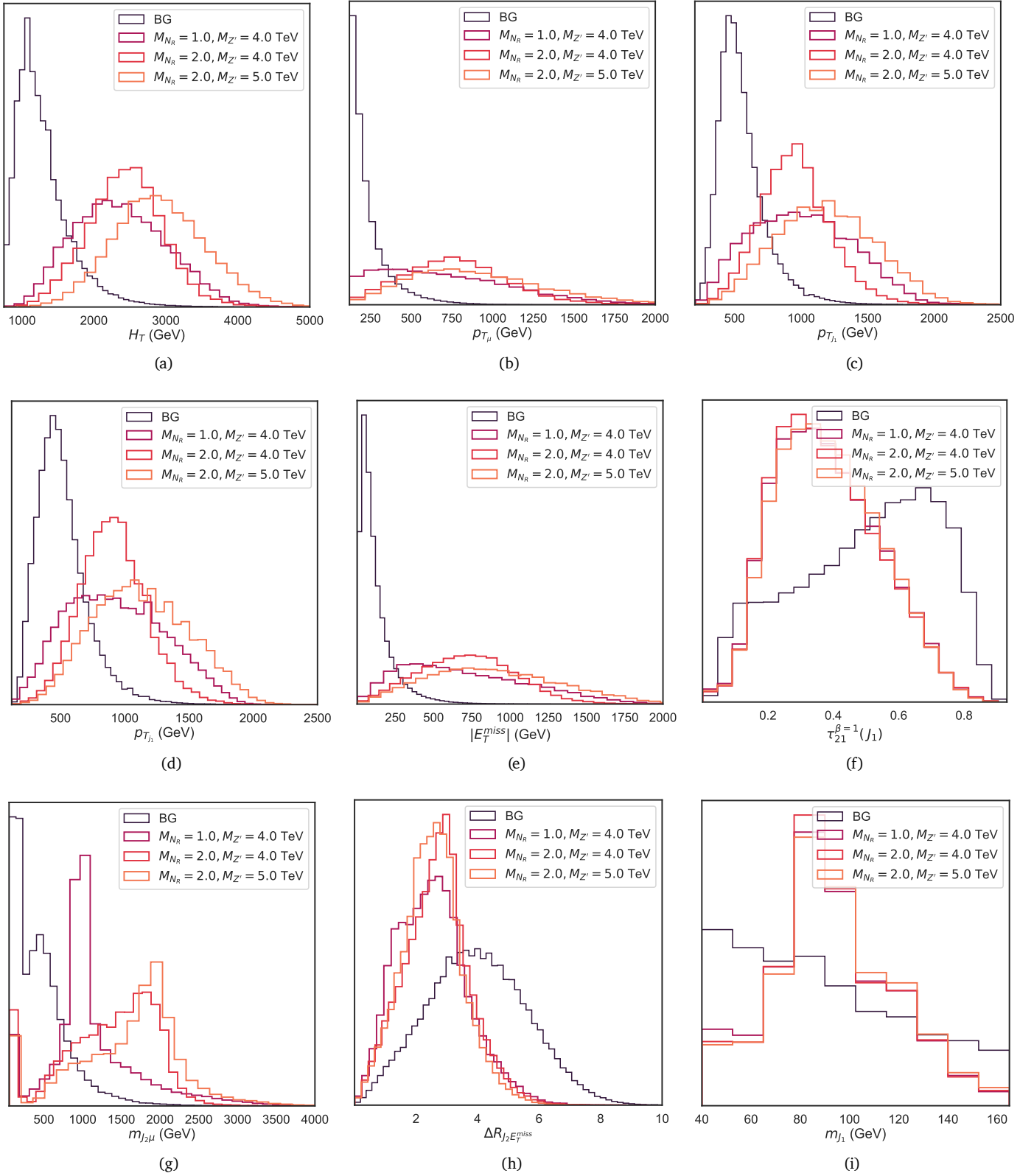


FIG. 2. Normalised density plots of the key features after passing through the cuts \mathcal{C}_1 to \mathcal{C}_5 for three benchmark points: (a) $M_{N_R} = 1$, $M_{Z'} = 4.0$ TeV, (b) $M_{N_R} = 2.0$, $M_{Z'} = 4.0$ TeV and (c) $M_{N_R} = 2.0$, $M_{Z'} = 5$ TeV. Here, all (fat-)jets are p_T -ordered.

TABLE IV. Projected number of events at the 14 TeV HL-LHC at different stages of analysis in the monolepton channel for $M_{N_R} = 2$ TeV, $M_{Z'} = 5$ TeV, and $g_z = 0.3$. For the signal, we assume a K factor of 1.3 [45].

	Signal	$t_h t_\ell$	$W_\ell + j$	$W_\ell W_h + j$	$Z_h W_\ell + j$	S/B
Initial	478	276832	392206	291684	22729	4.86×10^{-4}
\mathcal{C}_1	476	262336	379874	284631	22168	5.01×10^{-4}
\mathcal{C}_2	378	165693	271684	209542	16172	5.70×10^{-4}
\mathcal{C}_3	289	163771	221994	198316	15495	4.82×10^{-4}
\mathcal{C}_4	233	101175	95569	96647	7354	7.74×10^{-4}
\mathcal{C}_5	233	95707	89884	91762	6976	8.19×10^{-4}
DNN	227	~ 10	~ 122	~ 185	~ 11	0.69

given in Table V where J is used to denote a fatjet whereas j is used to identify an AK-4 jet.

We show the distributions of the key features of the signal and the background for three benchmark parameters in Fig. 2. The H_T (scalar sum of all hadronic objects) distributions show a clear separation between the signals and background due to the boosted nature of the final state, see Fig. 2(a). Moreover, for the signals, the transverse momentum distributions of the tagged muon, AK-4 jets, and the fatjet and the \cancel{E}_T distribution peak at considerably higher values than those of the background, see Figs. 2(b), 2(c), 2(d), 2(e). We also consider the n -subjettiness variables [51] which check for two-pronged (τ_2/τ_1) and three-pronged (τ_3/τ_2) nature of a fatjet for various values of β ($\beta \in \{1, 2, 3\}$). Since our fatjet parameters are tuned to identify a W -like (two-pronged) jet, the τ_2/τ_1 ratios are the key variables. Of these, the τ_2/τ_1 for $\beta = 2$ gives a clear separation between the signals and the background [Fig. 2(f)]. The τ_3/τ_2 ratios do not offer clear separations but, nevertheless, we include them due to the inclusive nature of the analysis cuts on the number of fatjets.

TABLE V. Kinematic variables chosen to analyse the monolepton signature; τ 's are the n -subjettiness ratios.

Variable	Description
H_T	Sum of transverse momenta of hadronic objects.
p_{T_i}	Transverse Momenta of all reconstructed objects.
\cancel{E}_T	Missing transverse energy.
m_{J_i}	Invariant Masses of the reconstructed fatjets.
ΔR_{ik}	Distances between any two reconstructed objects.
$m_{J,\mu}$	Invariant masses of the fatjet-lepton pairs.
$m_{j_i j_k}$	Invariant masses of any two reconstructed AK-4 jets.
$\tau_{21}^{\beta=1}$	τ_2/τ_1 , $\beta = 1.0$ for each fatjet.
$\tau_{21}^{\beta=2}$	τ_2/τ_1 , $\beta = 2.0$ for each fatjet.
$\tau_{32}^{\beta=1}$	τ_3/τ_2 , $\beta = 1.0$ for each fatjet.
$\tau_{32}^{\beta=2}$	τ_3/τ_2 , $\beta = 2.0$ for each fatjet.

The variable $m_{J,\ell}$ (invariant mass of a fatjet and the tagged muon) reconstructs the mass of the RHN very well—the trend can be clearly seen in Fig. 2(g). The $\Delta R_{J_i \cancel{E}_T}$ distributions in Fig. 2(h) can also distinguish the signals and the background well, as the final state objects come from the decay of an on-shell Z' . From the full set of kinematic variables, we drop the features that offer little separation between the signals and the background. For instance, we ignore the features $\Delta R_{J_1 j_1}$ and $\Delta R_{J_2 j_2}$ as we see that the leading (subleading) jet gets clustered inside the leading (subleading) fatjet for both signal and backgrounds. We also drop $\Delta R_{j_2 j_3}$, $m_{j_1 j_3}$ and $m_{j_2 j_3}$ as they show overlapping signal and background distributions. The final set of input features to the DNN model has 46 kinematic features.

D. Deep Learning model

To perform the classification task, we use a fully-connected DNN model which has an input layer, four hidden layers (with 50, 35, 30, and 10 nodes in the layers, respectively) and a single output layer. We implement the network using the TensorFlow module [52] and use a binary cross-entropy loss and the AdamW optimiser [53] with a learning rate 0.001 to train the network. We pick the benchmark point $(M_{Z'}, M_{N_R}) = (5.0, 2.0)$ TeV to optimise the hyperparameters using a grid search. The performance metric is the signal significance (\mathcal{S} score),

$$\mathcal{S} = \sqrt{2(N_S + N_B) \ln \left(\frac{N_S + N_B}{N_B} \right)} - 2N_S, \quad (14)$$

where N_S and N_B are the numbers of signal and background events allowed by the network at 3 ab^{-1} luminosity.

IV. RESULTS

In Fig. 3, we show the values of the $U(1)_z$ gauge coupling, g_z [Eq. (2)], needed to achieve the discovery (5σ) and exclusion ($\sim 2\sigma$) significance for a typical choice of parameters on the $M_{Z'} - M_{N_R}$ plane. To calculate the number of

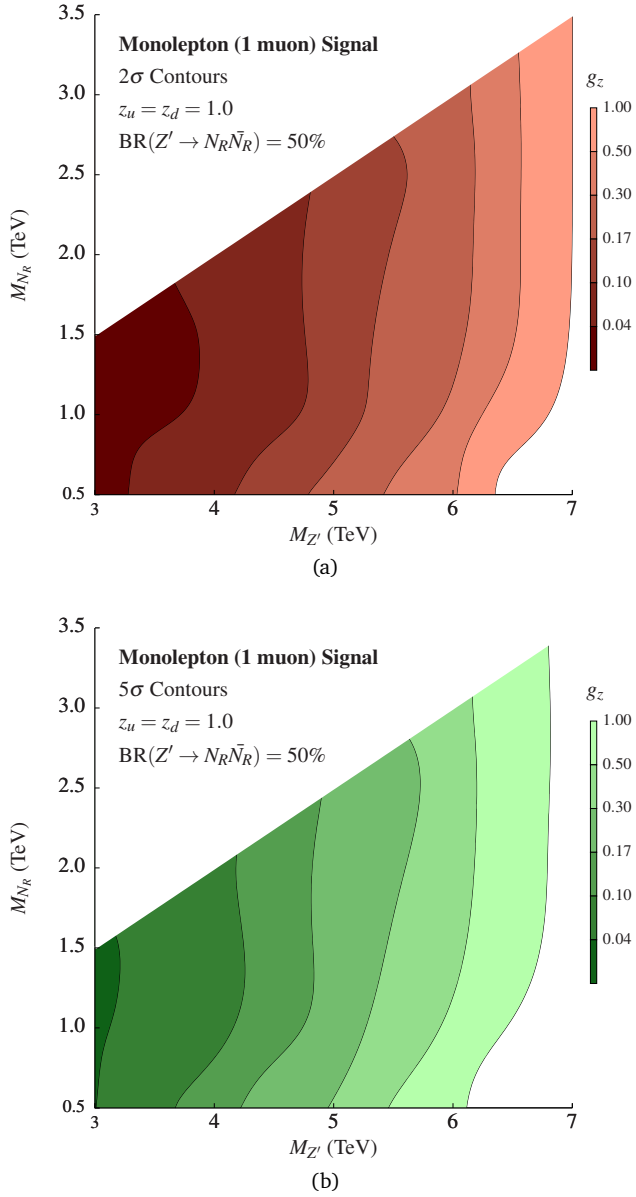


FIG. 3. The (a) exclusion ($\sim 2\sigma$) and (b) discovery (5σ) contours for the monolepton (1 muon) channel of $pp \rightarrow Z' \rightarrow N_R N_R$.

events, N_S and N_B , we use the final efficiencies of the DNN model at the working point with DNN response = 0.95. The g_z contours are broadly insensitive to the mass of the RHN. However, because of the high boosts, the event selection efficiency around $M_{N_R} = 0.5$ TeV (or less) is lower than those at larger values. Hence, one needs a larger g_z to achieve a high signal significance. This can be seen from the slightly deformed contours between $M_{N_R} = 1.0$ TeV and $M_{N_R} = 0.5$ TeV.

V. CONCLUSIONS

In this paper, we studied the prospects of a correlated search of a heavy neutral gauge boson Z' and the right-handed neutrino N_R in leptophobic $U(1)$ extensions. In particular, we analysed an experimentally unexplored channel $pp \rightarrow Z' \rightarrow N_R N_R$ where the N_R pair decays to a monolepton final state. Unlike the dilepton signature considered in our previous paper [23], probing the monolepton signature is highly challenging due to the huge background from SM processes which are hard to reduce with a cut-based analysis. Hence, in this paper, we used a DNN model to isolate the signal from the SM background, providing orders of magnitude gains in significance scores. We found that for $g_z \sim 0.7$, a Z' with mass up to 7 TeV can be discovered at the 14 TeV HL-LHC.

VI. ACKNOWLEDGEMENTS

C. N. acknowledges the Department of Science and Technology (DST)-Inspire for his fellowship. We also thank Jai Bardhan for helping us speed up the input-feature generation pipeline and for helpful discussions.

[1] P. Langacker, *Grand Unified Theories and Proton Decay*, *Phys. Rept.* **72** (1981) 185.
[2] D. London and J. L. Rosner, *Extra Gauge Bosons in E(6)*, *Phys. Rev. D* **34** (1986) 1530.
[3] J. L. Hewett and T. G. Rizzo, *Low-Energy Phenomenology of Superstring Inspired E(6) Models*, *Phys. Rept.* **183** (1989) 193.
[4] A. Leike, *The Phenomenology of extra neutral gauge bosons*, *Phys. Rept.* **317** (1999) 143–250, [[hep-ph/9805494](#)].
[5] P. Langacker, *The Physics of Heavy Z' Gauge Bosons*, *Rev. Mod. Phys.* **81** (2009) 1199–1228, [[0801.1345](#)].
[6] ATLAS collaboration, G. Aad et al., *Search for new resonances in mass distributions of jet pairs using 139 fb^{-1} of pp collisions at $\sqrt{s} = 13 \text{ TeV}$ with the ATLAS detector*,

JHEP **03** (2020) 145, [[1910.08447](#)].
[7] CMS collaboration, A. M. Sirunyan et al., *Search for high mass dijet resonances with a new background prediction method in proton-proton collisions at $\sqrt{s} = 13 \text{ TeV}$* , *JHEP* **05** (2020) 033, [[1911.03947](#)].
[8] ATLAS collaboration, G. Aad et al., *Search for high-mass dilepton resonances using 139 fb^{-1} of pp collision data collected at $\sqrt{s} = 13 \text{ TeV}$ with the ATLAS detector*, *Phys. Lett. B* **796** (2019) 68–87, [[1903.06248](#)].
[9] CMS collaboration, A. M. Sirunyan et al., *Search for resonant and nonresonant new phenomena in high-mass dilepton final states at $\sqrt{s} = 13 \text{ TeV}$* , *JHEP* **07** (2021) 208, [[2103.02708](#)].
[10] ATLAS collaboration, M. Aaboud et al., *Search for*

- resonances in diphoton events at $\sqrt{s}=13$ TeV with the ATLAS detector, *JHEP* **09** (2016) 001, [[1606.03833](#)].
- [11] CMS collaboration, V. Khachatryan et al., Search for high-mass diphoton resonances in proton–proton collisions at 13 TeV and combination with 8 TeV search, *Phys. Lett. B* **767** (2017) 147–170, [[1609.02507](#)].
- [12] ATLAS collaboration, G. Aad et al., Search for heavy diboson resonances in semileptonic final states in pp collisions at $\sqrt{s} = 13$ TeV with the ATLAS detector, *Eur. Phys. J. C* **80** (2020) 1165, [[2004.14636](#)].
- [13] CMS collaboration, A. Tumasyan et al., Search for heavy resonances decaying to WW, WZ, or WH boson pairs in the lepton plus merged jet final state in proton-proton collisions at $\sqrt{s} = 13$ TeV, *Phys. Rev. D* **105** (2022) 032008, [[2109.06055](#)].
- [14] CMS collaboration, V. Khachatryan et al., Search for resonant $t\bar{t}$ production in proton-proton collisions at $\sqrt{s} = 8$ TeV, *Phys. Rev. D* **93** (2016) 012001, [[1506.03062](#)].
- [15] A. Ferrari, Study of the production of a new Z' boson and its decay into Majorana neutrinos in pp collisions at $s = 14$ -TeV and in e^+e^- collisions at $s = 3$ -TeV, *Phys. Rev. D* **65** (2002) 093008.
- [16] A. Das, N. Okada and D. Raut, Enhanced pair production of heavy Majorana neutrinos at the LHC, *Phys. Rev. D* **97** (2018) 115023, [[1710.03377](#)].
- [17] A. Das, N. Okada and D. Raut, Heavy Majorana neutrino pair productions at the LHC in minimal $U(1)$ extended Standard Model, *Eur. Phys. J. C* **78** (2018) 696, [[1711.09896](#)].
- [18] P. Cox, C. Han and T. T. Yanagida, LHC Search for Right-handed Neutrinos in Z' Models, *JHEP* **01** (2018) 037, [[1707.04532](#)].
- [19] A. Das, S. Mandal, T. Nomura and S. Shil, Heavy Majorana neutrino pair production from Z' at hadron and lepton colliders, *Phys. Rev. D* **105** (2022) 095031, [[2202.13358](#)].
- [20] A. Ekstedt, R. Enberg, G. Ingelman, J. Löfgren and T. Mandal, Constraining minimal anomaly free $U(1)$ extensions of the Standard Model, *JHEP* **11** (2016) 071, [[1605.04855](#)].
- [21] G. K. Leontaris and J. Rizos, New fermion mass textures from anomalous $U(1)$ symmetries with baryon and lepton number conservation, *Nucl. Phys. B* **567** (2000) 32–60, [[hep-ph/9909206](#)].
- [22] A. Ekstedt, R. Enberg, G. Ingelman, J. Löfgren and T. Mandal, Minimal anomalous $U(1)$ theories and collider phenomenology, *JHEP* **02** (2018) 152, [[1712.03410](#)].
- [23] M. T. Arun, A. Chatterjee, T. Mandal, S. Mitra, A. Mukherjee and K. Nivedita, Search for the Z' boson decaying to a right-handed neutrino pair in leptophobic $U(1)$ models, *Phys. Rev. D* **106** (2022) 095035, [[2204.02949](#)].
- [24] D. Choudhury, K. Deka, T. Mandal and S. Sadhukhan, Neutrino and Z' phenomenology in an anomaly-free $U(1)$ extension: role of higher-dimensional operators, *JHEP* **06** (2020) 111, [[2002.02349](#)].
- [25] K. Deka, T. Mandal, A. Mukherjee and S. Sadhukhan, Leptogenesis in an anomaly-free $U(1)$ extension with higher-dimensional operators, *Nucl. Phys. B* **991** (2023) 116213, [[2105.15088](#)].
- [26] M. Thomas Arun, T. Mandal, S. Mitra, A. Mukherjee, L. Priya and A. Sampath, Testing left-right symmetry with an inverse seesaw mechanism at the LHC, *Phys. Rev. D* **105** (2022) 115007, [[2109.09585](#)].
- [27] A. Bhaskar, Y. Chaurasia, K. Deka, T. Mandal, S. Mitra and A. Mukherjee, Right-handed neutrino pair production via second-generation leptoquarks, *Phys. Lett. B* **843** (2023) 138039, [[2301.11889](#)].
- [28] R. N. Mohapatra, Mechanism for Understanding Small Neutrino Mass in Superstring Theories, *Phys. Rev. Lett.* **56** (1986) 561–563.
- [29] R. N. Mohapatra and J. W. F. Valle, Neutrino Mass and Baryon Number Nonconservation in Superstring Models, *Phys. Rev. D* **34** (1986) 1642.
- [30] D. Das, K. Ghosh, M. Mitra and S. Mondal, Probing sterile neutrinos in the framework of inverse seesaw mechanism through leptoquark productions, *Phys. Rev. D* **97** (2018) 015024, [[1708.06206](#)].
- [31] S. Jana, P. K. Vishnu and S. Saad, Minimal dirac neutrino mass models from $U(1)_R$ gauge symmetry and left–right asymmetry at colliders, *Eur. Phys. J. C* **79** (2019) 916, [[1904.07407](#)].
- [32] A. Das, S. Goswami, K. N. Vishnudath and T. Nomura, Constraining a general $U(1)'$ inverse seesaw model from vacuum stability, dark matter and collider, *Phys. Rev. D* **101** (2020) 055026, [[1905.00201](#)].
- [33] P. Bandyopadhyay, S. Jangid and M. Mitra, Scrutinizing Vacuum Stability in IDM with Type-III Inverse seesaw, *JHEP* **02** (2021) 075, [[2008.11956](#)].
- [34] A. Das, S. Goswami, V. K. N. and T. K. Poddar, Freeze-in sterile neutrino dark matter in a class of $U(1)'$ models with inverse seesaw, [2104.13986](#).
- [35] S. Banerjee, P. S. B. Dev, A. Ibarra, T. Mandal and M. Mitra, Prospects of Heavy Neutrino Searches at Future Lepton Colliders, *Phys. Rev. D* **92** (2015) 075002, [[1503.05491](#)].
- [36] S. Chakraborty, M. Mitra and S. Shil, Fat Jet Signature of a Heavy Neutrino at Lepton Collider, *Phys. Rev. D* **100** (2019) 015012, [[1810.08970](#)].
- [37] D. Barducci and E. Bertuzzo, The see-saw portal at future Higgs factories: the role of dimension six operators, *JHEP* **06** (2022) 077, [[2201.11754](#)].
- [38] K. S. Babu, C. F. Kolda and J. March-Russell, Leptophobic $U(1)$ s and the $R(b) - R(c)$ crisis, *Phys. Rev. D* **54** (1996) 4635–4647, [[hep-ph/9603212](#)].
- [39] J. L. Lopez and D. V. Nanopoulos, Leptophobic Z' in stringy flipped $SU(5)$, *Phys. Rev. D* **55** (1997) 397–406, [[hep-ph/9605359](#)].
- [40] T. G. Rizzo, Gauge kinetic mixing and leptophobic Z' in $E(6)$ and $SO(10)$, *Phys. Rev. D* **59** (1998) 015020, [[hep-ph/9806397](#)].
- [41] K. Leroux and D. London, Flavor changing neutral currents and leptophobic Z' gauge bosons, *Phys. Lett. B* **526** (2002) 97–103, [[hep-ph/0111246](#)].
- [42] P. Anastasopoulos, M. Bianchi, E. Dudas and E. Kiritsis, Anomalies, anomalous $U(1)$'s and generalized Chern-Simons terms, *JHEP* **11** (2006) 057, [[hep-th/0605225](#)].
- [43] P. Anastasopoulos, F. Fucito, A. Lionetto, G. Pradisi, A. Racioppi and Y. S. Stanev, Minimal Anomalous $U(1)$ -prime Extension of the MSSM, *Phys. Rev. D* **78** (2008) 085014, [[0804.1156](#)].
- [44] H. Hettmansperger, M. Lindner and W. Rodejohann, Phenomenological Consequences of sub-leading Terms in See-Saw Formulas, *JHEP* **04** (2011) 123, [[1102.3432](#)].
- [45] E. Eichten, I. Hinchliffe, K. D. Lane and C. Quigg, Super Collider Physics, *Rev. Mod. Phys.* **56** (1984) 579–707. [Addendum: *Rev.Mod.Phys.* **58**, 1065–1073 (1986)].

- [46] A. Alloul, N. D. Christensen, C. Degrande, C. Duhr and B. Fuks, *FeynRules 2.0 - A complete toolbox for tree-level phenomenology*, *Comput. Phys. Commun.* **185** (2014) 2250–2300, [[1310.1921](#)].
- [47] J. Alwall, R. Frederix, S. Frixione, V. Hirschi, F. Maltoni, O. Mattelaer et al., *The automated computation of tree-level and next-to-leading order differential cross sections, and their matching to parton shower simulations*, *JHEP* **07** (2014) 079, [[1405.0301](#)].
- [48] T. Sjöstrand, S. Ask, J. R. Christiansen, R. Corke, N. Desai, P. Ilten et al., *An introduction to PYTHIA 8.2*, *Comput. Phys. Commun.* **191** (2015) 159–177, [[1410.3012](#)].
- [49] **DELPHES 3** collaboration, J. de Favereau, C. Delaere, P. Demin, A. Giammanco, V. Lemaître, A. Mertens et al., *DELPHES 3, A modular framework for fast simulation of a generic collider experiment*, *JHEP* **02** (2014) 057, [[1307.6346](#)].
- [50] M. Cacciari, G. P. Salam and G. Soyez, *The anti- k_t jet clustering algorithm*, *JHEP* **04** (2008) 063, [[0802.1189](#)].
- [51] J. Thaler and K. Van Tilburg, *Identifying Boosted Objects with N -subjettiness*, *JHEP* **03** (2011) 015, [[1011.2268](#)].
- [52] M. Abadi, A. Agarwal, P. Barham, E. Brevdo, Z. Chen, C. Citro et al., *TensorFlow: Large-scale machine learning on heterogeneous systems*, 2015.
- [53] I. Loshchilov and F. Hutter, *Decoupled Weight Decay Regularization*, [1711.05101](#).